

# Power Optimization and Control in Wind Energy Conversion Systems Using Fractional Order Extremum Seeking

Jijin D H

M TECH Scholar, Electrical and Electronics, Lourdes Matha College of Science and Technology, Kerala, India

**Abstract** - Power optimization and control for grid-coupled wind energy conversion systems (WECS) has caught a big attention from early days. The methods widely used are model based power optimization algorithms as the outer loop and linear control methods in the inner loop. The method of extremum seeking control is a non model based optimization concept to extract maximum power from WECS in their subrated region. Induction generators are used widely in WECS since they are relatively inexpensive, robust and require a little maintenance. When operated using vector control techniques fast dynamic response and accurate torque control is obtained with the help of a matrix converter. In this paper, inner loop nonlinear control based on the principle of field oriented control (FOC) and feedback linearization is used along with maximum power point tracking (MPPT) in the outer loop. The proposed MPPT method is Fractional Order Extremum Seeking Control (FOESC). The convergence speed of FOESC is faster than the Integer Order ESC. Simulation results are presented to show the effectiveness of the proposed model.

**Key Words:** Non linear control systems, wind power generation, power control, adaptive systems, fractional order systems.

## 1. INTRODUCTION

A variable wind turbine (WT) generates power in subrated and rated power regions. In the subrated region Fig.2. region II, the maximum achievable turbine power is a function of the turbine speed at any velocity. The maximum power tracking algorithms developed in the recent are model dependent. They have the drawback that the controller needs to be redesigned for each wecs. A similar system is presented in [1] where fuzzy control is used. It works only for the specified fuzzy rules. Another method based on the speed sensorless power signal feedback (PSF) [2] uses lookup table values that are dependent on the system model and parameter values. There is another method of perturb and observe (P&O) [3] is more accurate but slow convergence. To overcome these difficulties, we present fractional order extremum seeking (FOES) algorithm which is non model based and with easily tunable design parameters. The FOESC has many advantages over ESC. A system with ESC is shown in [4] which shows slow convergence. The convergence speed is faster in FOESC hence transient response is improved.

The WECS uses Induction Generator (IG) which is relatively inexpensive, robust and require a little maintenance. They can respond relatively faster and more efficient to the variable wind speed. The stator of the IG is connected to a grid through a matrix converter (MC). The excitation or reactive power control required is fed from the grid itself by controlling the matrix converter. The stator frequency and stator voltage is varied through the MC to control the turbine speed. In order to implement field oriented control (FOC) and to improve transient response and robustness, an inner closed loop with a non linear controller is designed

Matrix Converter includes nine bidirectional switches operating in 27 different combinations. MCs provide bidirectional power flow, sinusoidal input/output currents, and controllable input power factor. Due to the absence of components with significant wear out characteristics (such as electrolytic capacitors), MC can potentially be very robust and reliable. The amount of space saved by an MC, when compared with a conventional back-to-back converter, has been estimated as a factor of three. Therefore, due to its small size, in some applications, the MC can be embedded in the machine.

## 2. WIND ENERGY CONVERSION SYSTEM

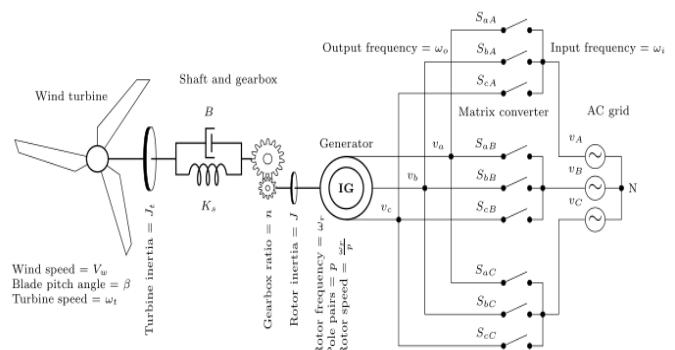


Fig-1 : WECS including IG,MC,turbine,gearbox and grid

The wind power available on the blade impact area is

$$P_w = 1/2 * \rho A V_w^3 \tag{1}$$

Where A is the blade area,  $\rho$  is the density of air and  $V_w$  is wind speed

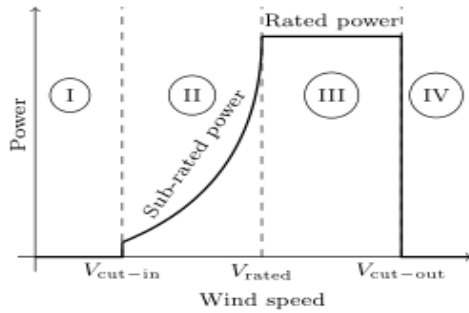


Fig-2 : Power curve including four operating regions

The turbine power can be derived from the power coefficient equation [4] is

$$P_t(V_w, w_t) = 55.115 \rho A \frac{((V_w/Rw_t) - 0.09)}{\exp((V_w/Rw_t) - 0.003)} V_w^3 \quad (2)$$

Where  $w_t$  is the turbine speed.

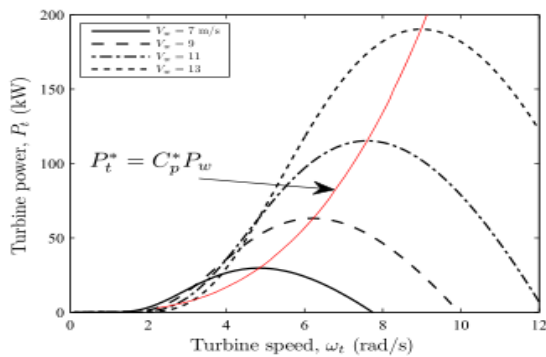


Fig-3 : Turbine power v/s turbine speed

Where  $P_t^*$  the optimal turbine is power and  $C_p^*$  is the optimal power coefficient.

Fig.3. shows the turbine power is optimal at points different for different wind speeds.

The WT shaft model is modeled as a spring damper. The dynamic equations of turbine, shaft and gearbox are

$$\frac{d\Theta^{\sim}}{dt} = w_t - w_r/pn, \quad \Theta^{\sim} = \Theta_t - \Theta_r/pn \quad (3)$$

$$\frac{d}{dt} w_t = 1/J_t * (-T_t - T_L), \quad T_t = P_t(V_w, w_t)/w_t \quad (4)$$

where  $w_r$  is the angular electrical frequency of the rotor of IG,  $\Theta_t$  is WT angular position,  $\Theta_r$  is the electrical angle of the rotor of IG,  $p$  is the number of pole pairs of the IG,  $n$  is the gearbox ratio,  $T_t$  is the turbine torque generated by the turbine power,  $T_L$  is the load torque created by the spring-damper model of the shaft and  $J_t$  is the turbine inertia coefficient.

$$T_L = K_s \Theta^{\sim} + B (w_t - w_r/pn) \quad (5)$$

where  $K_s$  is the stiffness coefficient of the spring and  $B$  is the damping ratio. The generator rotor angular speed equals  $w_r/p$

The block diagram of WECS is shown in fig.4.

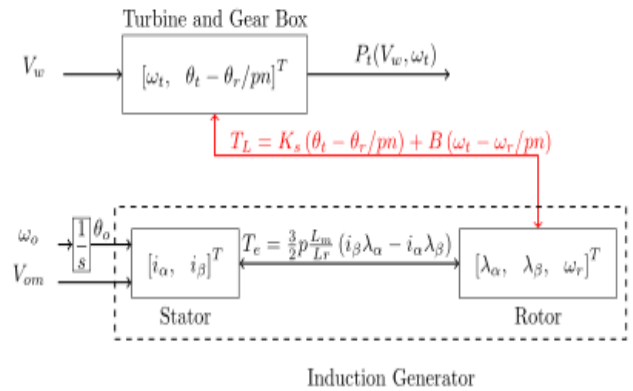


Fig-4 : Block diagram of WECS

The electromagnetic torque generated by IG is

$$T_e = \frac{3}{2} p \frac{L_m}{L_r} (i_\beta \lambda_\alpha - i_\alpha \lambda_\beta) \quad (6)$$

The state space dynamics of the WECS is

$$\frac{di_\alpha}{dt} = -a_0 i_\alpha + a_1 \lambda_\alpha + a_2 w_r \lambda_\beta + \frac{\cos \Theta_0}{L_s \sigma} V_{om} \quad (7)$$

$$\frac{di_\beta}{dt} = -a_0 i_\beta - a_2 w_r \lambda_\alpha + a_1 \lambda_\beta + \frac{\sin \Theta_0}{L_s \sigma} V_{om} \quad (8)$$

$$\frac{d}{dt} \lambda_\alpha = a_3 i_\alpha - a_4 \lambda_\alpha - w_r \lambda_\beta \quad (9)$$

$$\frac{d}{dt} \lambda_\beta = a_3 i_\beta - a_4 \lambda_\beta + w_r \lambda_\alpha \quad (10)$$

$$\frac{d}{dt} \Theta_0 = w_0 \quad (11)$$

$$\frac{d}{dt} w_r = \frac{3 * p^2 L_m}{2 * J L_r} (i_\beta \lambda_\alpha - i_\alpha \lambda_\beta) - \frac{p K_s}{n J} \Theta^{\sim} - \frac{p B}{n J} (w_t - \frac{w_r}{pn}) \quad (12)$$

$$\frac{d\Theta^{\sim}}{dt} = (w_t - \frac{w_r}{pn}) \quad (13)$$

$$\frac{d}{dt} w_t = -\frac{P_t(V_w, w_t)}{w_t J_t} - \frac{K_s}{J_t} \Theta^{\sim} - \frac{B}{J_t} (w_t - \frac{w_r}{pn}) \quad (14)$$

Where  $w_0$  and  $\Theta_0$  are the stator or output electrical frequency and stator electrical angle of the IG  $V_{om}$  is the amplitude of the output voltage,  $i_\alpha$  and  $i_\beta$  are stator currents.

$\lambda_\alpha$  and  $\lambda_\beta$  are rotor flux linkages,  $L_m$  is the mutual inductance,  $L_s = L_{ls} + L_m$  is stator inductance,  $L_r = L_{lr} + L_m$  is rotor inductance and  $\sigma = 1 - L_m^2 / (L_s * L_r)$ .

### 3. OVERALL SYSTEM

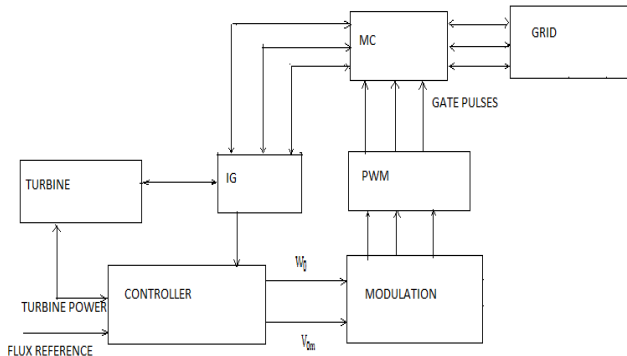


Fig-5 : overall system including controller

The turbine power is measured from the equation(2) is given to the outer loop controller that is FOESC which gives an approximated value of the optimal turbine speed with respect to Fig.2. It is then given to the inner loop nonlinear control. The non linear control used here is feedback linearization which performs FOC and avoids magnetic saturation of the IG. It is a closed loop drives the turbine speed to the optimal value found by the MPPT and drives the rotor flux to the reference flux value given manually. The conventional FOC control method with P&O method is shown in [5] and [6]. The PI controller used causes high response time and high overshooting if error is unexpectedly very high. It is also difficult to design PI since unpredictable variations in the machine parameters, external load disturbance and non linear dynamics. The other methods used for FOC concept are Fuzzy logic, gain scheduled PI and relative gain array. The feedback linearization gives a faster response and desired response can be obtained by adjusting the feedback gains. The controller gives stator frequency and stator voltage given to modulation, the modulation and pulse generation for MC can be referred from [4],[7] and [8]. The MC regulates the stator electrical frequency to control the turbine speed. The stator voltage amplitude can be maintained to regulate the rotor flux. The turbine speed variation does not affect rotor flux. Similarly the rotor flux reference can be varied even independently of reference optimal speed found by the MPPT. This is an improvement over FOC.

*Remark1:* The torque-speed characteristic of an induction machine is normally quite steep in the neighborhood of stator electrical frequency (synchronous speed)  $w_0$ , and so the electrical rotor speed  $w_r$ , will be near the synchronous speed. This means that changing the reference value of the turbine speed  $w_t$  which translates in variation of the electrical rotor speed eventually results in changing the stator electrical frequency [9]. Thus, by controlling the

stator electrical frequency, one can approximately control the turbine speed or vice versa.

### 4. CONTROLLER DESIGN

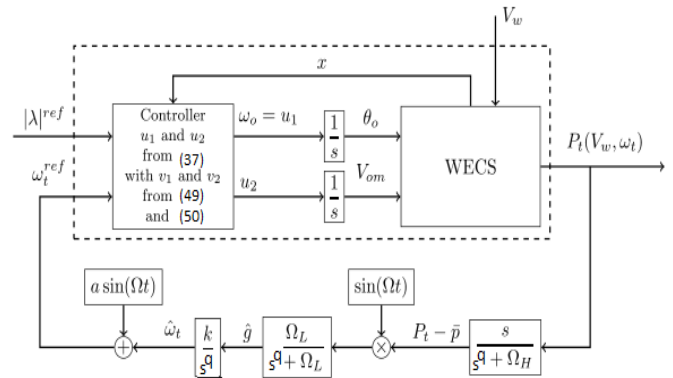


Fig-6 : WECS with FOESC and inner loop nonlinear control.

Where  $x_{i(i=1 \text{ to } 9)} = [i_\alpha, i_\beta, \lambda_\alpha, \lambda_\beta, \Theta_0, V_{om}, w_0, \Theta, w_t]^T$

When flux amplitude  $\sqrt{(\lambda_\alpha^2 + \lambda_\beta^2)}$ , is regulated to a constant reference value, and considering the fact that the dynamics of  $w_t$  are considerably slower than the electrical dynamics, we can assume that the dynamics are linear, but during flux transient, the system has nonlinear terms and it is coupled. This method can be improved by achieving exact input-output decoupling and linearization via a nonlinear state feedback that is not more complex than the conventional FOC [10].

From (2) and Fig.3, we know that the turbine speed controls the power generation. In addition, we are interested in decoupling the rotor flux and electromagnetic torque to obtain the benefits of FOC. For these reasons, we introduce turbine speed,  $y_1 = w_t$  and flux amplitude,  $\eta_1 = |\lambda|^2$ , as measurable outputs. For future analysis, we assume that the power coefficient and wind speed function satisfy following assumption.

Assumption 1: The power coefficient  $C_p(w_t, V_w)$  and wind speed function  $V_w(t)$  are bounded  $C^3$  functions with bounded derivatives. Hence, the mechanical torque  $T_t$  is a bounded  $C^3$  function with bounded derivatives.

Based on the selected outputs and having Assumption 1 satisfied, we apply feedback linearization with the following change of variables to WECS dynamics:

$$y_1 = \Psi_1(x) = w_t \tag{15}$$

$$y_2 = L_f^{-1} \Psi_1(x) = -a_9(x_9 - \frac{x_7}{p_n}) - a_8 x_8 - \frac{T_t}{J_t} \tag{16}$$

$$y_3 = L_f^2 \Psi_1(x) = b_0 \xi_q + b_1 L_f \Psi_1(x) + b_2 x_8 + b_3 \frac{T_t}{J_t} - \frac{\dot{T}_t}{J_t} \quad (17)$$

$$y_4 = L_f^3 \Psi_1(x) = b_4 L_f^2 \Psi_1(x) + b_5 L_f \Psi_1(x) + b_6 x_8 - \frac{b_0}{L_s \sigma} x_6 \lambda_q - x_7 (b_7 \Psi_2(x) + b_8 L_f \Psi_2(x)) + b_9 \frac{T_t}{J_t} - b_{10} \frac{\dot{T}_t}{J_t} - \frac{\ddot{T}_t}{J_t} \quad (18)$$

$$\eta_1 = \Psi_2(x) = x_3^2 + x_4^2 \quad (19)$$

$$\eta_2 = L_f \Psi_2(x) = 2a_3 \xi_d - 2a_4 \Psi_2(x) \quad (20)$$

$$\eta_3 = L_f^2 \Psi_2(x) = b_{12} \Psi_2(x) - b_{11} L_f \Psi_2(x) + b_{13} x_7 (L_f^2 \Psi_1(x) - b_1 L_f \Psi_1(x) - b_2 x_8 - b_3 \frac{T_t}{J_t} + \frac{\dot{T}_t}{J_t}) + 2a_3^2 i_s + \frac{2a_3}{L_s \sigma} x_6 \lambda_d \quad (21)$$

$$\Delta = x_8 \quad (22)$$

$$\Phi = \arctan\left(\frac{x_4}{x_3}\right) \quad (23)$$

Where  $\xi_d = x_1 x_3 + x_2 x_4$ ,  $\xi_q = x_2 x_3 - x_1 x_4$ ,  $i_s = i_\alpha^2 + i_\beta^2$  and

$$\begin{bmatrix} \lambda_d \\ \lambda_q \end{bmatrix} = \begin{bmatrix} \cos x_5 & \sin x_5 \\ -\sin x_5 & \cos x_5 \end{bmatrix} \begin{bmatrix} x_3 \\ x_4 \end{bmatrix} \quad (24)$$

The change of variables results in the following equations,

$$y_2 = \dot{y}_1 \quad (25)$$

$$y_3 = \dot{y}_2 \quad (26)$$

$$y_4 = \dot{y}_3 \quad (27)$$

$$y_4 = G_1 + \frac{b_0 \lambda_d}{L_s \sigma} x_6 u_1 - \frac{b_0 \lambda_q}{L_s \sigma} u_2 \quad (28)$$

$$\eta_2 = \dot{\eta}_1 \quad (29)$$

$$\eta_3 = \dot{\eta}_2 \quad (30)$$

$$\dot{\eta}_3 = G_2 + \frac{2a_3 \lambda_d}{L_s \sigma} x_6 u_1 - \frac{2a_3 \lambda_q}{L_s \sigma} u_2 \quad (31)$$

$$\dot{\Delta} = -\frac{y_2}{a_9} - \frac{a_8}{a_9} \Delta - \frac{T_t}{a_9 J_t} \quad (32)$$

$$\dot{\Phi} = w_r + \frac{a_3}{b_0 \eta_1} (y_3 - b_1 y_2 - b_2 \Delta - b_3 \frac{T_t}{J_t} + \frac{\dot{T}_t}{J_t}) \quad (33)$$

Where  $u_1$  is the stator electrical frequency  $w_0$  and  $u_2$  is the voltage amplitude rate. (32) and (33) are zero dynamics of the system

$$G_1 = b_4 y_4 + b_5 y_3 - y_2 \frac{b_6}{a_9} - \frac{a_8 b_6}{a_9} \Delta - \frac{b_0 x_6}{L_s \sigma} (a_3 i_d - a_4 \lambda_q + x_7 \lambda_d) - x_7 (b_7 \eta_1 + b_8 \eta_2) - x_7 (b_7 \eta_2 + b_8 \eta_3) - \frac{b_6 T_t}{a_9 J_t} + b_9 \frac{\dot{T}_t}{J_t} + b_{10} \frac{\ddot{T}_t}{J_t} - \frac{\ddot{T}_t}{J_t} \quad (34)$$

$$G_2 = -b_{11} \eta_3 + b_{12} \eta_2 + b_{13} x_7 \xi_q + b_{13} x_7 (y_4 - b_1 y_3 - b_2 x_8 - b_3 \frac{\dot{T}_t}{J_t} + \frac{\ddot{T}_t}{J_t}) + 4a_3^2 (a_1 \xi_d - a_0 i_s - \frac{2x_6}{L_s \sigma} i_d) + \frac{2a_3}{L_s \sigma} x_6 (a_3 i_d - a_4 \lambda_d - x_7 \lambda_q) \quad (35)$$

Where

$$\begin{bmatrix} i_d \\ i_q \end{bmatrix} = \begin{bmatrix} \cos x_5 & \sin x_5 \\ -\sin x_5 & \cos x_5 \end{bmatrix} \begin{bmatrix} x_1 \\ x_2 \end{bmatrix} \quad (36)$$

Defining control signals as

$$\begin{bmatrix} x_6 u_1 \\ u_2 \end{bmatrix} = \frac{L_s \sigma}{\sqrt{\eta_1}} \begin{bmatrix} \cos(\Phi - \theta_0) & \sin(\Phi - \theta_0) \\ -\sin(\Phi - \theta_0) & \cos(\Phi - \theta_0) \end{bmatrix} \begin{bmatrix} \frac{v_1 - G_1}{b_0} \\ \frac{v_2 - G_2}{2a_3} \end{bmatrix} \quad (37)$$

Applying another step of change of variables

$$z = [y_1 - w_{tref}, y_2, y_3, y_4]^T \quad (38)$$

$$\zeta = [\eta_1 - (|\lambda|_{ref})^2, \eta_2, \eta_3]^T \quad (39)$$

$$z_2 = \dot{z}_1 \quad (40)$$

$$z_3 = \dot{z}_2 \quad (41)$$

$$z_4 = \dot{z}_3 \quad (42)$$

$$v_1 = \dot{z}_4 \quad (43)$$

$$\zeta_2 = \dot{\zeta}_1 \quad (44)$$

$$\zeta_3 = \dot{\zeta}_2 \quad (45)$$

$$v_2 = \dot{\zeta}_3 \quad (46)$$

$$\dot{\Delta} = -\frac{z_2}{a_9} - \frac{a_8}{a_9} \Delta - \frac{T_t}{a_9 J_t} \quad (47)$$

$$\dot{\Phi} = w_r + \frac{a_3}{b_0 \eta_1} (z_3 - b_1 z_2 - b_2 \Delta - b_3 \frac{T_t}{J_t} + \frac{\dot{T}_t}{J_t}) \quad (48)$$

Linear state feedback,

$$v_1 = -z_1 k_1' - z_2 k_2' - z_3 k_3' - z_4 k_4' \quad (49)$$

$$v_2 = -\zeta_1 k_1'' - \zeta_2 k_2'' - \zeta_3 k_3'' \quad (50)$$

By appropriate selection of the feedback gains in (49) and (50) and using (37), we can obtain the desired closed-loop response time. The controller drives the turbine speed  $w_t$  towards the reference value  $w_{tref}$  found by MPPT while amplitude of rotor flux  $\lambda$  has converged to its desired

value  $|\lambda|_{ref}$ . The values of  $a_i$  and  $b_i$  values are given in appendix.

### 5. MPPT Using FOESC

Assumption 2: The following holds for the turbine power map around its MPP for  $V$  cut-in  $<V < V$  rated (see Fig. 3) where  $w_t^*$  is the optimal turbine speed

$$\frac{\partial P_t(V_w, w_t)}{\partial w_t}(w_t^*) = 0 \tag{51}$$

$$\frac{\partial}{\partial w_t} \frac{\partial P_t(V_w, w_t)}{\partial w_t}(w_t^*) < 0 \tag{52}$$

Where  $w_t^*$  is the optimal turbine speed

ESC is a branch of adaptive control. The ES scheme estimates the gradient of the cost function  $P_t$ , by injecting a small perturbation, a  $\sin(\Omega t)$ , which is very slow with respect to the dynamics of the controller system and its amplitude is enough small in comparison with  $w_t$ . The high-pass filter removes the dc part of the signal. The multiplication of the resulting signal by  $\sin(\Omega t)$  creates an estimate of the gradient of the cost function, which is smoothed using a low-pass filter. When  $w_t$  is larger than its optimal value, the estimate of the gradient  $g^{\wedge}$ , is negative and causes  $w_t$  to decrease. On the other hand, when  $w_t$  is smaller than  $w_t^*$ , then  $g^{\wedge} > 0$ , which increases  $w_t$  toward  $w_t^*$ .

In general,

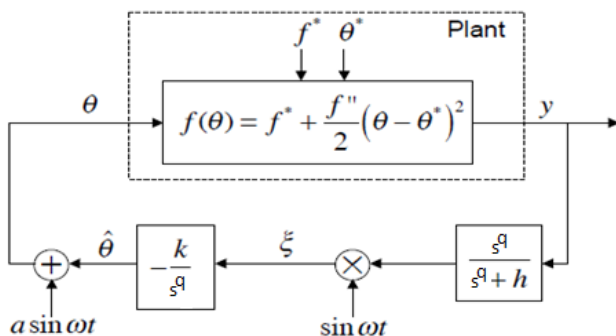


Fig-7 : The FOESC in a general case

The plant dynamics can be written as

$$y = f^* + f''(\Theta(t) - \Theta^*) \tag{53}$$

Considering cost function  $f$  to be minimized and assuming  $f'$  is positive, The error,

$$\Theta^{\sim} = \Theta^* - \Theta^{\wedge} \tag{54}$$

$$\Theta(t) - \Theta^* = \Theta^{\wedge}(t) + a \sin(\omega t) - \Theta^* = a \sin(\omega t) - \Theta^{\sim}(t) \tag{55}$$

Substituting in (53)

$$Y = f'' + \frac{a^2 f''}{4} + \frac{f''}{2} \Theta^{\sim 2} - a f'' \Theta^{\sim} \sin(\omega t) + \frac{a^2 f''}{4} \cos(2\omega t) \tag{56}$$

The quadratic terms can be neglected

The high pass filter eliminates the dc components and the output obtained is

$$\frac{s^q}{s^q + h}[y] = -a f'' \Theta^{\sim} \sin(\omega t) + \frac{a^2 f''}{4} \cos(2\omega t) \tag{57}$$

$$\xi = \sin(\omega t) \frac{s^q}{s^q + h}[y] \tag{58}$$

$$\xi = \frac{-a^2 f''}{4} \Theta^{\sim} + \frac{a^2 f''}{4} \Theta^{\sim} \cos(2\omega t) + \frac{a^2 f''}{8} (\sin(\omega t) - \sin(3\omega t)) \tag{59}$$

The integrator attenuates the high frequency terms. Taking derivative  $D^q$  of eqn (54) gives

$$D^q \Theta^{\sim} = -D^q \Theta^{\wedge} \tag{60}$$

Also

$$\xi = D^q \Theta^{\wedge} \tag{61}$$

$$s^q \Theta^{\sim}(s) = \frac{-ka^2 f''}{4} \Theta^{\sim}(s) \tag{62}$$

It is clear that the rate of error convergence depends on integral gain  $k$ , perturbing signal amplitude  $a$  and perturbing frequency  $1/w$  when taking time scale  $T = wt$ .

$$\frac{d^q}{dT} \Theta^{\sim} = \frac{-ka^2 f''}{4w} \Theta^{\sim} \tag{63}$$

The stability of FOESC based on averaging and jacobian can be referred from [11]

The averaged linearized model of the FOESC in fig.7. can be obtained from [12] is given as,

$$\frac{\Theta^{\sim}}{\Theta^*} = \frac{\lambda(\lambda^2 + 2h\lambda + h^2 + w^2)}{(\lambda^3 + (2h + ka^2)\lambda^2 + (h^2 + w^2 + ka^2h)\lambda + ka^2w^2)} \tag{64}$$

Where  $\lambda = s^q$

The convergence of the FOESC can be verified by checking the boundary stability of the root locus of integer order IOESC and fractional order FOESC of the general system in fig.8.



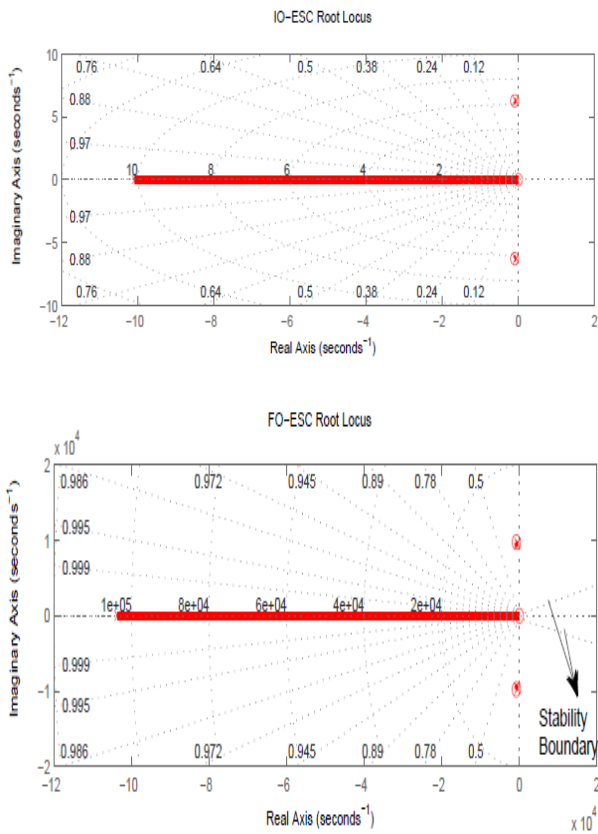


Fig-8 : .root locus of IOESC and FOESC

It can be seen that the stability boundary is increased for FOESC. The stability boundary condition is  $\text{Arg}(\text{eig}(A)) > \frac{q\pi}{2}$  where  $A$  is the state space matrix of the eqn (64). In the fig.8, the eigen values of the IOESC system is near the imaginary axis hence it has slowly damped poles but the eigen values of FOESC system is not close to the stability boundary of the system hence they can be damped faster. The conditions for choosing parameters for the system given in fig.6 are as follows.

According to eqn (63) , the convergence speed depends on the order( $a^2$ ) hence  $a$  should be sufficiently small. But a higher value of  $a$  causes residual error and a very lower value causes not to attain global stability. Perturbation signal frequency  $w$  can be chosen sufficiently large. Since integral gain  $k$  is the learning rate, it must be higher than the period of perturbation  $w \gg k$  so that it converges faster. The value of high pass filter frequency can be chosen to eliminate dc component can be a lower value. Similarly the value of low pass filter frequency is chosen so that avoiding high frequency terms for the averaging of integral.

The order of the FOESC  $q$  must be chosen carefully because lower the order, the limiting (boundary) value of gain increases which affects the convergence. Hence a quadratic error term between turbine power after the FOESC and directly measured power is taken and plotted for different

values of fractional order (0.3 to 1.3).The optimal fractional order can be obtained corresponding to minimum error.

$$J_q = \sum_{k=0}^N (P(k\Delta)_{\text{tfoesc}} - (P(k\Delta)_{\text{tm}})^2 \tag{65}$$

$N$  is the width of the working time window and  $\Delta$  is the time sampling rate

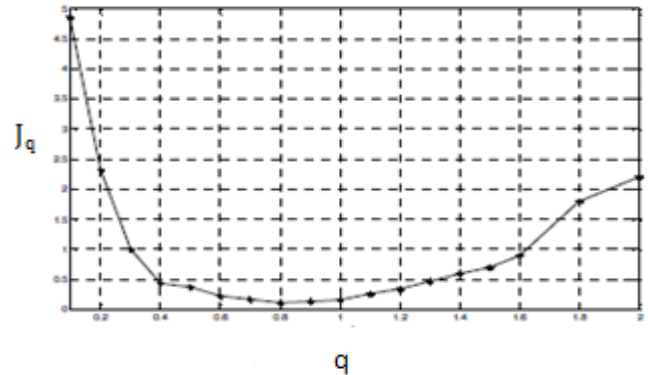


Fig-9 : Quadratic error v/s fractional order

## 6. SIMULATION RESULT

Control signals are designed such that the poles of  $z$ -error subsystem (40)–(43) and  $\zeta$ -error subsystems (44)–(46) move to  $P_z = [-550 - 600 - 650 - 700]$  and  $P_\zeta = [-570 - 620 - 670]$ , respectively. The response time of the closed-loop system is about 20 ms, which is 25 times faster than the open-loop system. We select the parameters of the FOES loop of fig 6 as follows:  $W = 100$  rad/s,  $\Omega_1 = 6$  rad/s,  $\Omega_h = 5$  rad/s,  $a = 0.1$  and  $k = 0.004$ . The optimal value of order  $q$  is found to be 0.8 from the fig.9. The wind speed tracking of IOESC and FOESC is shown in fig 10 for a wind speed of Gaussian signal 20m/s avg

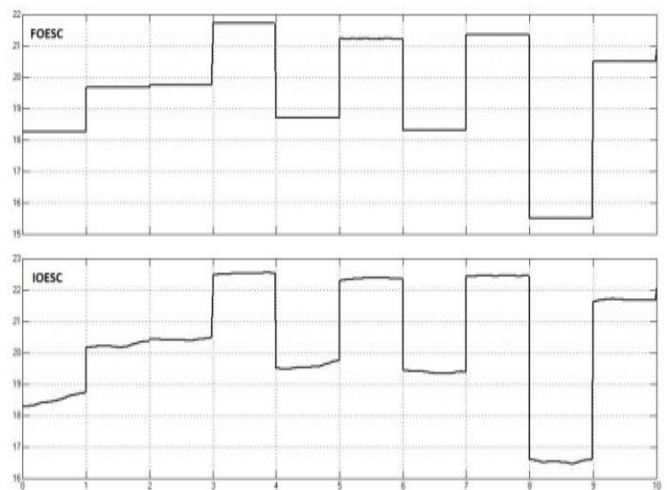


Fig-10 : wind speed tracking of IOESC and FOESC of the proposed system

The power tracking can be found more in FOESC in fig 11

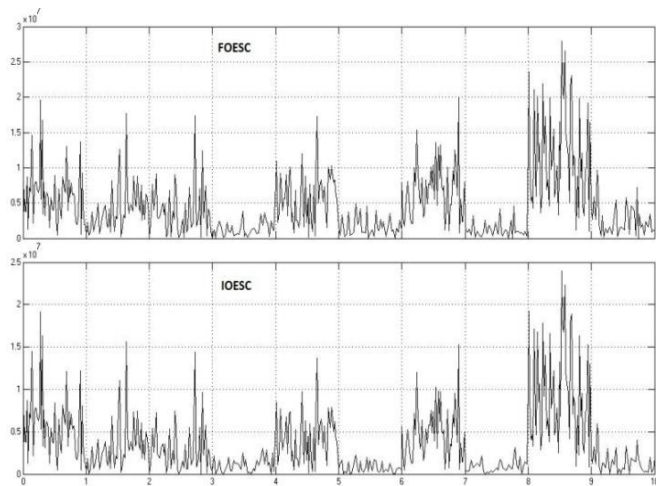


Fig-11 : power tracking for a wind speed of 20m/s

The power tracked by the FOESC is found more than IOESC. Thus FOESC is more efficient for maximum power tracking. The efficiency and improvement of transient response when including inner non linear controller can be verified fom [4].

### 7. CONCLUSION

The system employed FOESC to extract maximum power from the available wind power. The design employed an inner loop non linear controller based on FOC and feedback linearization to control the closed loop transient response with respect to the optimal turbine speed tracked by FOESC. It provides perfect input output decoupling and better than conventional FOC which increases performance robustness with respect to system parameters. Also the control strategy prevents magnetic saturation of the IG. The optimization algorithm can readily be extended to other classes of WECS without major changes. The main parameters to be adjusted are probing frequency and amplitude of the perturbing signal. A comparison is done with IOESC and FOESC is found better tracking of optimal turbine speed and power. It results in higher efficiency and since the WECS runs for a long period of time, a small improvement in power efficiency guarantees extracting a higher energy level and leads to cost reduction.

### APPENDIX

TABLE-1 : Definition of Parameters and Their Numerical Values

Blade length R	10m
Blade pitch angle	0
Air density ρ	1.25Kg/ m <sup>3</sup>
Turbine inertia J <sub>t</sub>	100 Kg m <sup>2</sup>
Gear box ratio	20

Stiffnes coefficient K <sub>s</sub>	2*10 <sup>6</sup> Nm/rad
Damping coefficient B	5*10 <sup>5</sup> Nm/rad/s
No of pole pairs of SCIG	2
Stator leakage inductance L <sub>ls</sub>	3.2 mH
Rotor leakage inductance L <sub>lr</sub>	3.2 mH
Magnetizing inductance L <sub>m</sub>	143.36 mH
Moment of inertia of SCIG J	11.06 Kg m <sup>2</sup>
Stator resistance R <sub>s</sub>	0.262 Ω
Rotor resistance R <sub>r</sub>	0.187 Ω

TABLE -2 : Constant Parameters

a <sub>0</sub>	$a_2 a_3 + R_s / (\sigma L_s)$	b <sub>0</sub>	$a_5 a_9 / (pn)$
a <sub>1</sub>	$a_2 a_4$	b <sub>1</sub>	$a_8 / a_9 + a_7 / (pn) - a_9$
a <sub>2</sub>	$L_m / (\sigma L_s L_r)$	b <sub>2</sub>	$a_8^2 / a_9$
a <sub>3</sub>	$L_m R_r / L_r$	b <sub>3</sub>	$a_8 / a_9 + a_7 / (pn)$
a <sub>4</sub>	$R_r / L_r$	b <sub>4</sub>	$b_1 - a_0 - a_4$
a <sub>5</sub>	$3p^2 L_m / (2J L_r)$	b <sub>5</sub>	$a_0 b_1 + a_4 b_1 - b_2 / a_9$
a <sub>6</sub>	$p K_s / (J n)$	b <sub>6</sub>	$a_0 b_2 + a_4 b_2 - a_8 b_2 / a_9$
a <sub>7</sub>	$p B / (J n)$	b <sub>7</sub>	$a_2 b_0 + a_4 b_0 / a_3$
a <sub>8</sub>	$K_s / J_t$	b <sub>8</sub>	$b_0 / (2a_3)$
a <sub>9</sub>	$B / J_t$	b <sub>9</sub>	$a_0 b_3 + a_4 b_3 - b_2 / a_9$
b <sub>12</sub>	$2a_1 a_3 - 2a_0 a_4 - 2a_4^2$	b <sub>10</sub>	$b_3 - a_0 - a_4$
b <sub>13</sub>	$2a_3 / b_0$	b <sub>11</sub>	$a_0 + 3a_4$

### ACKNOWLEDGEMENT

Foremost, I would like to express my sincere gratitude to my advisor Assistant Professor Swapna M of Lourdes Matha College of Science and Technology(LMCST) Trivandrum Kerala India for the continuous support of my MTech thesis study and research, for her patience, motivation, enthusiasm and immense knowledge. Her guidance helped me in all the time of research and writing of this thesis.

Besides my advisor, I would like to thank respected HOD Dr.Mohanalin Rajarakthnam and all the teachers of Electrical and Electronics department LMCST for their encouragement, motivation and help.

Last but not the least, I would like to thank my family; my parents and my brother for supporting me to complete this thesis successfully.

### REFERENCES

[1] T. Senjyu, R. Sakamoto, N. Urasaki, T. Funabashi, H. Fujita, and H. Sekine, "Output power leveling of wind turbine generator for all operating regions by pitch angle control," IEEE Trans. Energy Convers., vol. 21, no. 2, pp. 467-475, Jun. 2006.

[2] S. M. Barakati, M. Kazerani, and J. D. Aplevich, "Maximum power tracking control for a wind turbine system including a matrix converter," IEEE Trans. Energy Convers., vol. 24, no. 3, pp. 705-713, Sep. 2009

- [3] S. M. R. Kazmi, H. Goto, H.-J. Guo, and O. Ichinokura, "A novel algorithm for fast and efficient speed-sensorless maximum power point tracking in wind energy conversion systems," *IEEE Trans. Ind. Electron.*, vol. 58, no. 1, pp. 29–36, Jan. 2011.
- [4] Azad Ghaffari, Miroslav Krstić, "Power Optimization and Control in Wind Energy Conversion System using Extremum Seeking", *IEEE Trans. Control Systems*, vol. 22, no. 5, pp.1684 – 1695, Sep. 2014.
- [5] R. Cardenas, R. Pena, J. Clare, and P. Wheeler, "Analytical and experimental evaluation of a WECS based on a cage induction generator fed by a matrix converter," *IEEE Trans. Energy Convers.*, vol. 26, no. 1, pp. 204–215, Mar. 2011.
- [6] B. Wu, Y. Lang, N. Zargari, and S. Kouro, *Power Conversion and Control of Wind Energy Systems*. New York, NY, USA: Wiley, 2011.
- [7] Vinod Kumar, R. R. Joshi, and R. C. Bansa, "Optimal Control of Matrix-Converter-Based WECS for Performance Enhancement and Efficiency Optimization" *IEEE Trans. Energy Convers.*, Vol 24, no. 1, March 2009.
- [8] S. M. Barakati, M. Kazerani, and J. D. Aplevich, "Maximum power tracking control for a wind turbine system including a matrix converter," *IEEE Trans. Energy Convers.*, vol. 24, no. 3, pp. 705–713, Sep. 2009.
- [9] P. C. Krause, O. Wasynczuk, and S. D. Sudhoff, *Analysis of Electric Machinery and Drive Systems*. New York, NY, USA: Wiley, 2002.
- [10] R. Marino, S. Peresada, and P. Valigi, "Adaptive input-output linearizing control of induction motors," *IEEE Trans. Autom. Control*, vol. 38, no. 2, pp. 208–221, Feb. 1993.
- [11] Hadi Malek, Sara Dadras, YangQuan Chen, "An Improved Maximum Power Point Tracking Based on Fractional Order Extremum Seeking Control in Grid-Connected Photovoltaic Systems" *IDETC, CIE* Portland, Oregon, USA Aug 4-7, 2013
- [12] Hadi Malek, "Control of Grid-Connected Photovoltaic Systems using Fractional Order Operators" *UTAH STATE UNIVERSITY* Logan, Utah 2014
- [12] A. I. Bratcu, E. C. Iulian Munteanu, and S. Epure, "Energetic optimization of variable speed wind energy conversion systems by extremum seeking control," in *Proc. Int. Conf. Comput. Tool*, 2007, pp. 2536–2541.
- [13] L. Huber and D. Borojevic, "Space vector modulated three-phase to three-phase matrix converter with input power factor correction," *IEEE Trans. Ind. Appl.*, vol. 31, no. 6, pp. 1234–1246, Nov./Dec. 1995.
- [14] K. E. Johnson, L. Y. Pao, M. J. Balas, and L. J. Fingersh, "Control of variable-speed wind turbines: Standard and adaptive techniques for maximizing energy capture," *IEEE Control Syst. Mag.*, vol. 26, no. 3, pp. 70–81, Jun. 2006.
- [15] L. Y. Pao and K. E. Johnson, "Control of wind turbines," *IEEE Control Syst. Mag.*, vol. 31, no. 1, pp. 44–62, Feb. 2011.
- [16] M. Komatsu, H. Miyamoto, H. Ohmori, and A. Sano, "Output maximization control of wind turbine based on extremum control strategy," in *Proc. Amer. Control Conf.*, 2001, pp. 1739–1740.
- [17] M. Krstić and H.-H. Wang, "Stability of extremum seeking feedback for general nonlinear dynamic systems," *Automatica*, vol. 36, no. 4, pp. 595–601, 2000.
- [18] R. Marino, S. Peresada, and P. Valigi, "Adaptive input-output linearizing control of induction motors," *IEEE Trans. Autom. Control*, vol. 38, no. 2, pp. 208–221, Feb. 1993.
- [19] T. Pan, Z. Ji, and Z. Jiang, "Maximum power point tracking of wind energy conversion systems based on sliding mode extremum seeking control," in *Proc. IEEE Energy Conf.*, Nov. 2008, pp. 1–5.
- [20] Y. Tan, D. Nešić, and I. Mareels, "On non-local stability properties of extremum seeking control," *Automatica*, vol. 42, pp. 889–903, Jun. 2006.

## BIOGRAPHIES



JIJIN D H now working as Adhoc Assistant Professor at College of engineering and Management Punnapra Kerala India in the EEE Dept. Completed MTech from Lourdes Matha College of Science and Technology Trivandrum in Control Systems. Completed BTech from Govt Engineering College Barton Hill Trivandrum India in Electrical and Electronics Engineering